

# Use of GOES-R Advanced Baseline Imager (ABI) Proxy Data to Assess the Performance of the GOES-R Winds Algorithm

Jaime Daniels<sup>1</sup>, Wayne Bresky<sup>2</sup>, Andrew Bailey<sup>2</sup>, Americo Allegrino<sup>2</sup>, Steven Wanzong<sup>3</sup>, Chris Velden<sup>3</sup>

1. NOAA/NESDIS Center for Satellite Applications and Research, NOAA Science Center, College Park, Maryland 20740, U.S.A.
2. I.M. Systems Group (IMSG), Rockville, Maryland 20852, U.S.A.
3. Cooperative Institute for Meteorological Satellite Studies (CIMSS), Space Science and Engineering Center (SSEC), University of Wisconsin – Madison, Wisconsin 53706, U.S.A

## Abstract

A new Atmospheric Motion Vector (AMV) nested tracking algorithm has been developed for the Advanced Baseline Imager (ABI) to be flown on NOAA's future GOES-R satellite which is scheduled to be launched in November 2016. GOES-N/O/P, Meteosat SEVERI, Terra/Aqua MODIS, NOAA/AVHRR, METOP/AVHRR, and NPP/VIIRS imagery have served as GOES-R ABI proxy data sources for the continued development, testing, and validation of the GOES-R AMV algorithms. Himawari-8 was successfully launched October 7, 2014 and carries the Advanced Himawari Imager (AHI) which is an almost identical instrument to the ABI. The availability of AHI datasets brings an unprecedented opportunity to exercise and test the GOES-R AMV algorithm.

This paper focuses on the outcome of our work to assess the performance of the nested tracking algorithm using H-8/AHI imagery as well as the other proxy data sources noted above. We will share what we have learned since developing the baseline algorithm and discuss algorithm improvements we have developed and tested.

## STATUS OF GOES-R

GOES-R is scheduled to be launched in November 2016. GOES-R will carry the Advanced Baseline Imager (ABI) (Schmit et al, 2016). The ABI is a state-of-the-art 16-band radiometer, with spectral bands covering the visible, near-infrared and infrared portions of the electro-magnetic spectrum. Many attributes of the ABI, such as spectral, spatial, and temporal resolution, radiometrics, and image navigation/registration are much improved from the current series of GOES imagers. The number of spectral bands increases from 5 to 16, the coverage rate improves by a factor of five and the spatial resolution improves by a factor of 4 (two in each direction). Table 1 provides information on the ABI spectral bands. Highlighted in gray are those bands used to track features (ie., clouds or moisture gradients in clear sky conditions) and derive estimates of atmospheric motion.

Two ABI scan modes will be operationally supported. Figure 1 shows an illustration of the different sectors that will be scanned. The first scan mode is Scan Mode 3 where a full disk scan will be completed every 15 minutes, a Continental United States (CONUS) scan will be completed every 5 minutes, and a Mesoscale (MESO) scan completed every minute (assuming two MESO sectors) or 30 seconds (assuming one MESO sector). The second scan mode is Scan Mode 4 where the full disk is scanned continuously every 5 minutes. AMVs will be derived at varying cadences - Every

hour over the Full Disk, every 5 minutes over the CONUS sector, and every 5 minutes over the MESO sector from an image triplet for each of these sectors.

**Table 1.** Summary of GOES-R ABI spectral bands. Bands used to derive atmospheric motion winds are highlighted in gray.

ABI Band	Approximate Central Wavelength ( $\mu\text{m}$ )	Sub-point pixel spacing	Descriptive Name
1	0.47	1	"Blue"
2	0.64	0.5	"Red"
3	0.864	1	"Veggie"
4	1.373	2	"Cirrus"
5	1.61	1	"Snow/Ice"
6	2.24	2	"Cloud Particle Size"
7	3.90	2	"Shortwave window"
8	6.19	2	"Upper-level Water Vapor"
9	6.93	2	"Mid-Level Water Vapor"
10	7.34	2	"Lower/Mid-level Water Vapor"
11	8.44	2	"Cloud-top Phase"
12	9.61	2	"Ozone"
13	10.33	2	"Clean longwave window"
14	11.21	2	"Longwave window"
15	12.29	2	"Dirty longwave window"
16	13.28	2	"CO <sub>2</sub> "

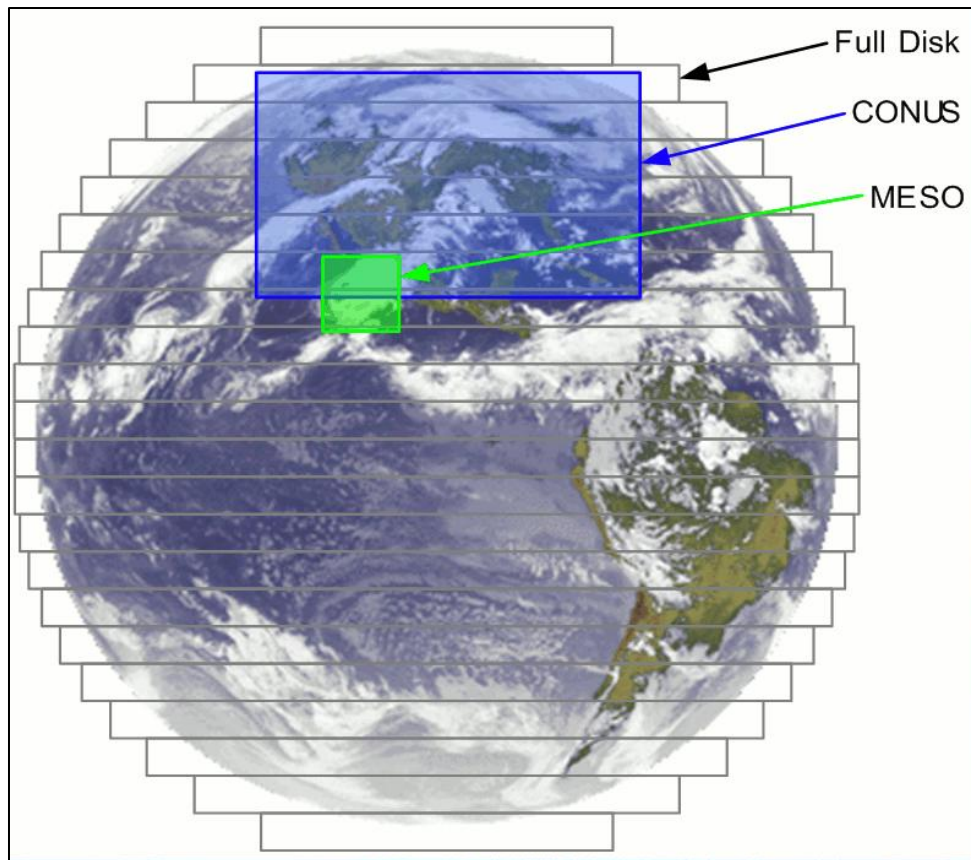


**Figure 1.** Various sectors that the GOES-R ABI will scan and take observations over.

The Post-Launch Test (PLT) period to check out, validate, and characterize the performance of the GOES-R instruments and Level-2 derived products (ie., AMVs, cloud products, etc) will occur over a 6 month period. Following this PLT period, there will be another 6 month period of extended validation where further validation and characterization of the instrument and Level-2 products will be performed.

### **GOES-R WINDS ALGORITHM**

The GOES-R winds algorithm uses a nested tracking approach (Bresky et al, 2012; Daniels 2010) that involves deriving a motion estimate for all possible 5x5 pixel sub-target regions “nested” within a larger target window that produces a field of local motion vectors associated with each target window. The Sum-of-Squared Differences (SSD) correlation method is used to track features in time. A clustering algorithm (Ester et al, 1996) is subsequently applied to the field of local motion vector displacements in order to extract coherent motion clusters within the target window. The dominant motion in the target scene is determined from the largest motion cluster. This process is illustrated in Figure 2. The presence of smaller, coherent motion clusters indicate motions that differ from the dominant motion either in scale and/or because it comes from a different level in the atmosphere. Sometimes a smaller coherent motion cluster represents some motion that has nothing to do with the instantaneous wind (ie., the movement of a frontal boundary). Using the apriori knowledge of cloud height (Heidinger, 2014; Heidinger, 2010; Heidinger and Pavolonis, 2009) at each pixel belonging to the largest cluster enables the assignment of a height (in hPa) to the derived wind vector.

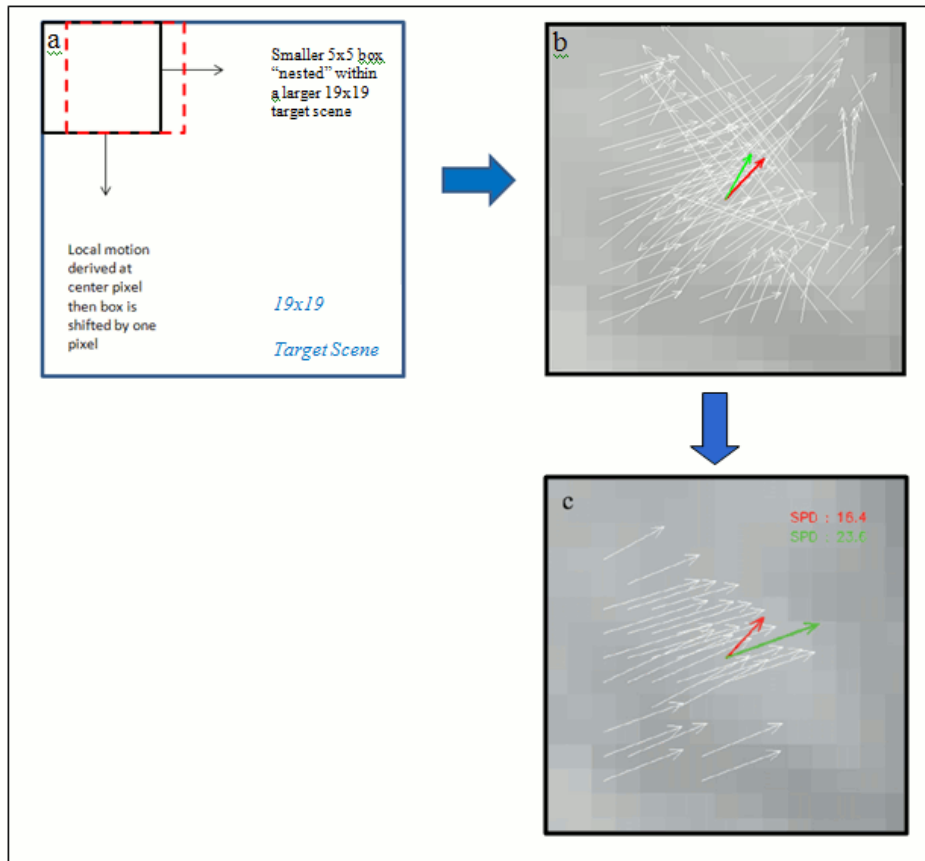


**Figure 2.** (a). Smaller target scenes “nested” within a larger target scene. (b) An example of the local motion field derived with nested tracking. The white vectors show the local motion derived with a 5x5 box centered on the pixel location. The average motion of all local vectors is shown in green and the vector derived by tracking the entire scene is shown in red. Note that local motion vectors are not generated near the boundary where a full 5x5 box does not exist. (c) Local vectors in white belonging to the largest cluster. The green arrow represents the mean vector of the local vectors belonging to the largest cluster. The red arrow represents the motion of the larger target scene.

## USING AVAILABLE ABI PROXY DATA IN PREPARATION FOR GOES-R

Numerous satellite sensors were used and served as GOES-R ABI proxy data (See Table 2) for the development and validation of the GOES-R algorithms which included the winds algorithm and algorithms (e.g., Clear sky mask, cloud type/phase, cloud top temperature/pressure) whose output the winds algorithm depends on. Most of the early development of the GOES-R algorithms utilized data from EUMETSAT’s Meteosat Second Generation (MSG) SEVIRI instruments (Schmetz et al, 2002). Figure 3 shows examples of the Meteosat-10/SEVIRI winds derived from the GOES-R algorithms.

The successful launch of JMA’s Himawari-8 satellite and the availability of Advanced Himawari-8 Imager (AHI) data (Beshho et al, 2014), provided us with an unprecedented opportunity to exercise and validate the GOES-R algorithms given that the AHI instrument is almost identical to the GOES-R ABI. Figure 4 shows examples of the Himawari-8/AHI winds derived from the GOES-R algorithms. The higher spatial resolution of the imagery lends itself to a significant increase in the number of processed targets and good AMVs as compared to the heritage GEO satellite instruments. This is especially true for generating winds from the 0.5km visible data. Table 3 shows the typical number of

**Table 2.** Proxy data applied to the GOES-R Algorithms

Satellite/Sensor	Notes
Meteosat-8/9/10 SEVIRI	Most of our early algorithm development work was done with these sensors
GOES-13/15	Operational Target Date: Spring 2017
GOES-14	Super Rapid Scans for GOES-R Readiness
Himawari-8/AHI	Ideal ABI proxy data source; recent work focused on these data
NOAA-15/18/19 AVHRR	Operational Target Date: Spring 2017
METOP-A/B AVHRR	Operational Target Date: Spring 2017
Terra/Aqua MODIS	Operational Target Date: Spring 2017
Soumi NPP/VIIRS	Operational: May 2014

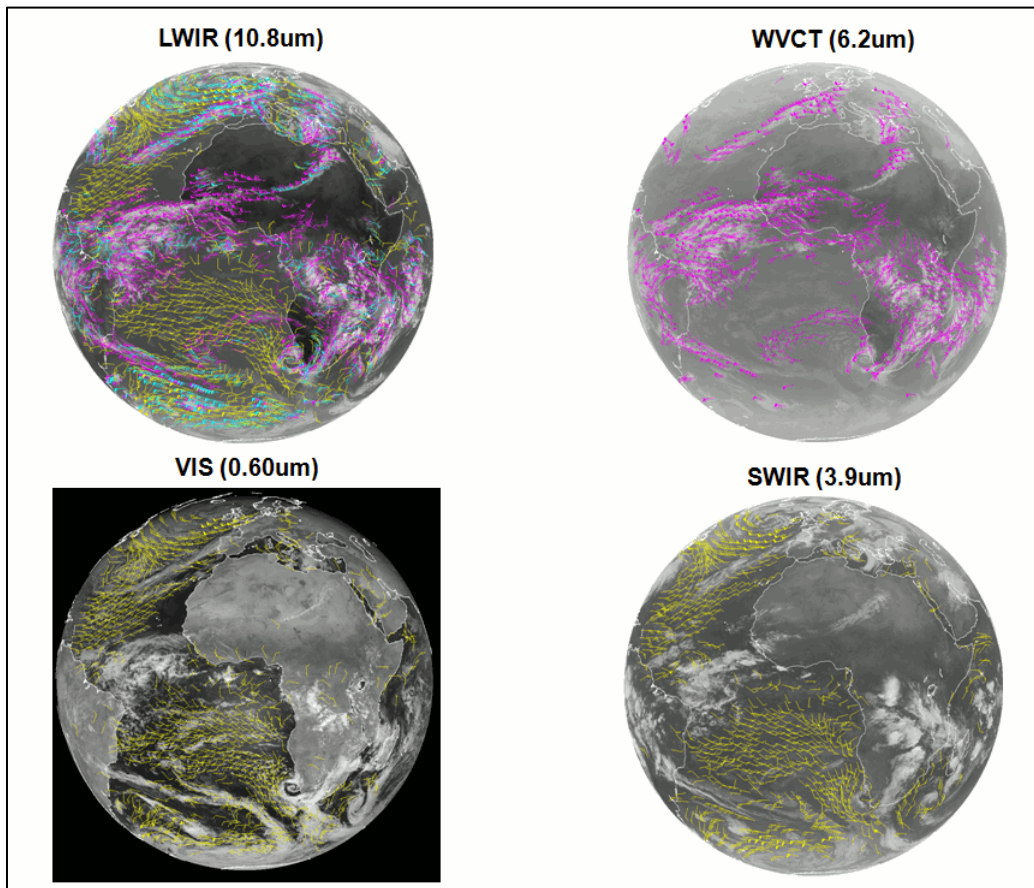


**Figure 3.** Meteosat-10/SEVIRI winds derived from the GOES-R algorithms. High level (100-400 hPa) winds are plotted in magenta, mid-level (400-700 hPa) are plotted in cyan, and low level (below 700 hPa) are plotted in yellow.



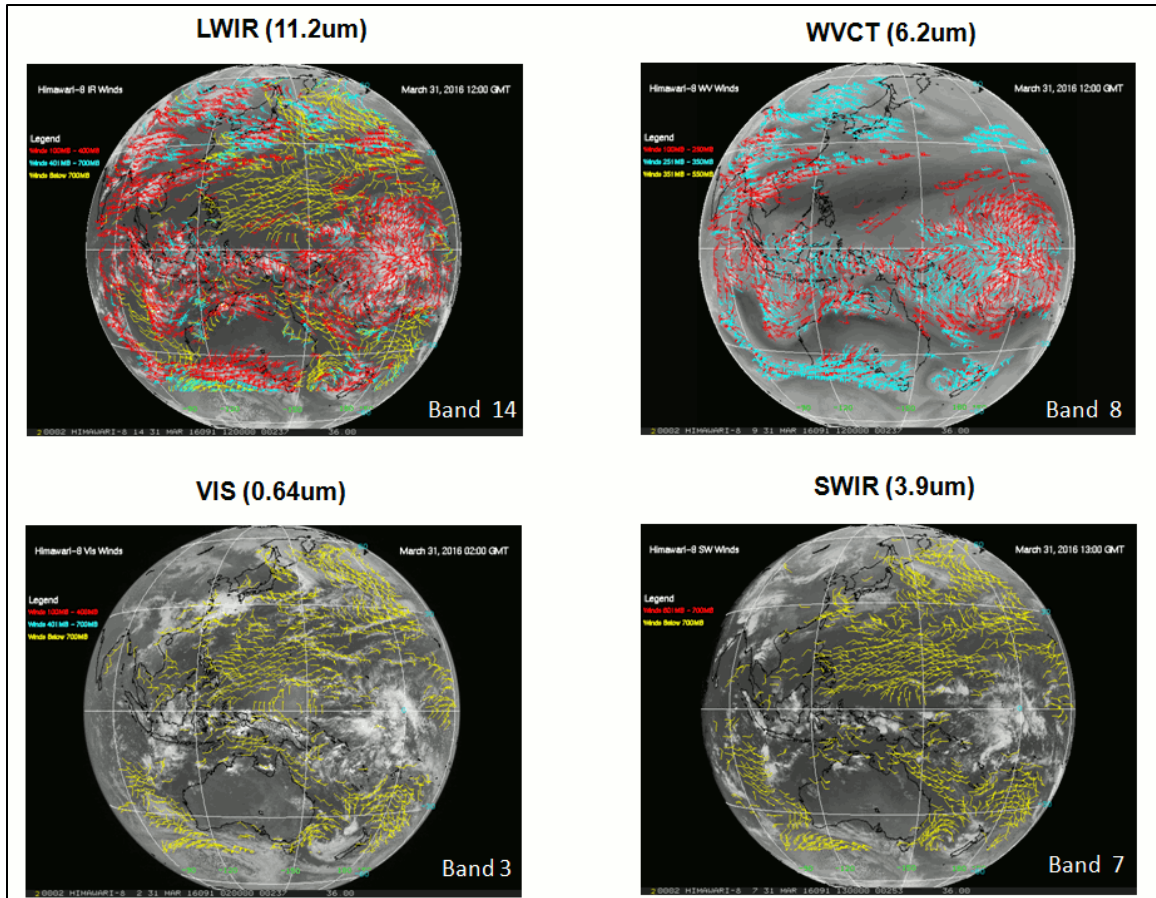


**Figure 4.** Himawari-8/AHI winds derived from the GOES-R algorithms. High level (100-400 hPa) winds are plotted in magenta, mid-level (400-700 hPa) are plotted in cyan, and low level (below 700 hPa) are plotted in yellow. Not all winds are plotted in these figures for the sake of readability.

good H-8 winds that are generated over the full disk via the GOES-R algorithms and accompanying processing configuration. For GOES-R we expect similar AMV counts and coverage (geographical and vertical) as indicated in Table 3 and Figure 4.

The quality of the H-8 winds was assessed by comparing the retrieved AMVs to collocated radiosonde winds. Table 4 shows comparison statistics for various wind types over various pressure layers (all, high, mid, low). The AMVs were generated over the entire full disk domain using successive images separated by a 10 minute time interval. The comparison metrics indicate that the quality of satellite AMVs are generally quite good. Disconcerting is the magnitude of the slow bias associated with the LWIR (11um) AMVs at mid levels. This is being investigated.

In order to get a sense of the quality of the H-8 AMV height assignments, a Level-of-Best Fit assessment was performed using collocated rawinsonde vertical wind profiles. Figure 5 shows the level of best-fit profiles of RMSE and absolute speed bias at 200 hPa, 300 hPa, 500 hPa, and 700 hPa for the nested tracking H-8 winds derived from 10.8um imagery for the period 9 February – 15 June 2016. Inspection of Figure 5 indicates that minimums in the level-of-best-fit (RMSE and Bias) curves match the AMV assigned heights quite well with the minimums in the RMSE and speed bias profile curves occurring about 25 hPa below the assigned AMV pressure level at each of the levels except for 300 hPa. This result suggests that the heights associated with these AMVs are assigned slightly too high up in the atmosphere.

**Table 3.** Proxy data applied to the GOES-R Algorithms

Wind Type	Typical Number of Good Winds over FD	Acceptable Vertical Coverage (hPa)
Visible (Band 3; 0.64um)	100,000	Below 700
SWIR (Band 7; 3.9um)	20,000	Below 700
WV Cloud-top (Band 8; 6.2um)	30,000	Above 350
WV Clear-Sky (Band 8; 6.2um)	5,000	100-1000
WV Clear-Sky (Band 9; 7.0um)	5,000	100-1000
WV Clear-sky (Band 10; 7.3um)	1,000	450-700
LWIR (Band 14; 11um)	50,000	100-1000

**Table 4.** Himawar-8/AHI AMV/rawinsonde comparison statistics for various wind types.

All Levels (100-1000 hPa)	12/22/15 – 1/4/16	10/29/15 – 1/4/16	8/13/15 – 1/4/16	8/13/15 – 1/4/16
	LWIR (11.2um)	WVCT (6.2um)	VIS (0.65 um)	SWIR (3.9um)
MVD (m/s)	5.71	5.57	3.21	3.22
St. Deviation (m/s)	4.76	4.43	2.16	2.21
Speed bias (m/s)	-0.97	-0.09	0.05	-0.19
Speed (m/s)	19.28	23.66	8.88	8.99
Sample	24004	169943	16420	34719
<b>High Level (100-400 hPa)</b>	<b>LWIR</b>	<b>WVCT</b>		
MVD (m/s)	6.16	5.57		
St. Deviation (m/s)	4.96	4.43		
Speed bias (m/s)	-0.65	-0.09		
Speed (m/s)	24.31	23.66		
Sample	11637	169943		
<b>Mid Level (400-700 hPa)</b>	<b>LWIR</b>			
MVD (m/s)	7.39			
Precision (m/s)	5.48			
Speed bias (m/s)	-1.93			
Speed (m/s)	20.28			
Sample	5689			
<b>Low Level (700-1000 hPa)</b>	<b>LWIR</b>		<b>VIS</b>	<b>SWIR</b>
MVD (m/s)	3.51		3.21	3.22
St. Deviation (m/s)	2.28		2.16	2.21
Speed bias (m/s)	-0.72		0.05	-0.19
Speed (m/s)	9.66		8.88	8.99
Sample	6678		16420	34719

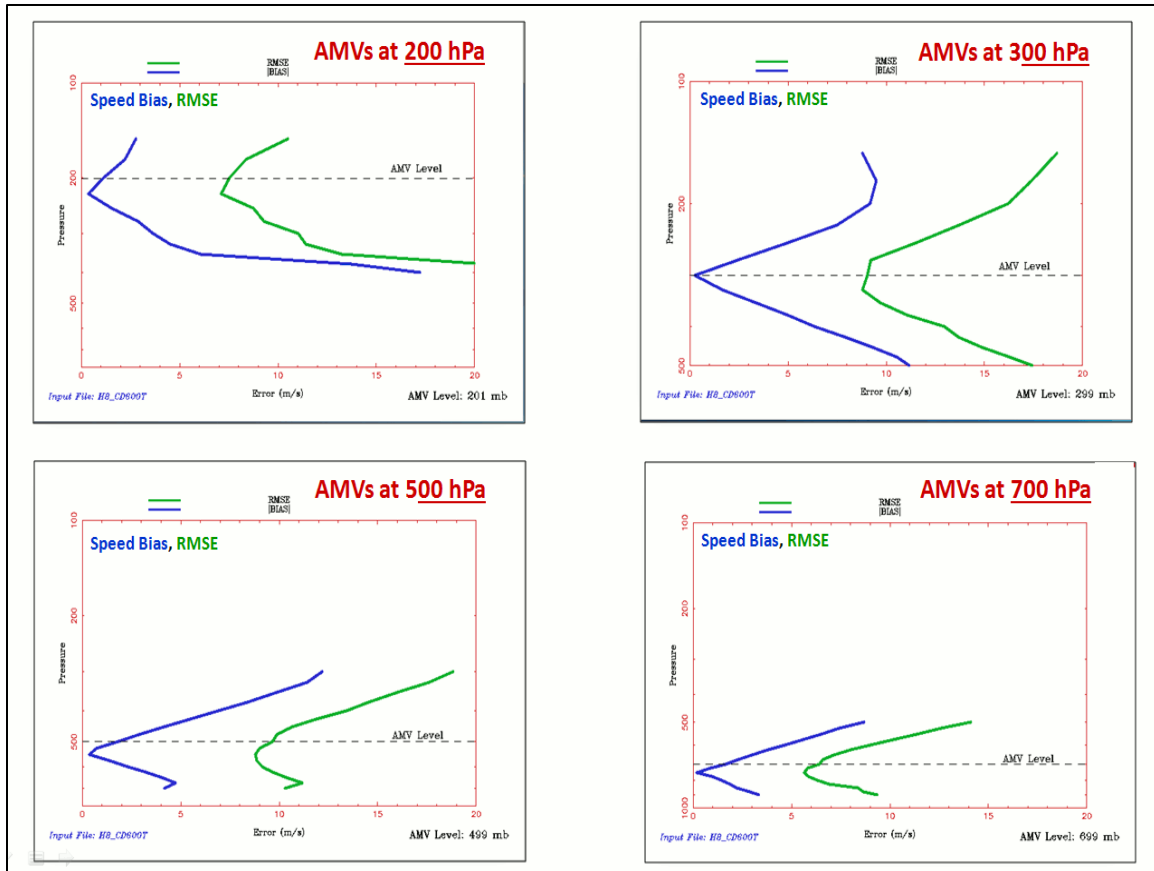


**Figure 5.** Level of best-fit profiles of RMSE (green) and absolute speed bias (blue) at 200 hPa, 300 hPa, 500 hPa, and 700 hPa nested tracking winds derived from Himawari-8/AHI 10.8um imagery for the period 9 February – 15 June 2016.

## CASE STUDIES AND LESSONS LEARNED USING RAPID SCAN IMAGERY

Recently we have focused on performing case studies involving the use of rapid scan imagery from GOES-14 and Himawari-8. In the case of GOES-14 we used 1-min imagery over Hurricane Sandy and in the case of Himawari-8 we used 2.5 minute data over Super Typhoon Soudelor. Our focus areas for these studies included optimizing the geographic coverage of the winds product, using the full resolution (0.5km) H-8 0.64um visible channel for feature tracking, optimizing the use of temporal imagery, optimizing the target scene size and spacing, and quality control. So for example, given a set of imagery, what is the optimal configuration to use to generate AMVs in a tropical cyclone environment? What winds scale(s) are trying to be captured? Our overarching goals are to provide AMVs with good and consistent geographic coverage and to improve wind analyses, NWP forecasts, and the utilization and impact of the AMV product in the end-to-end forecast process.

Our first close look at visible AMVs derived from GOES-14 rapid scan imagery around Hurricane Sandy revealed large gaps in geographic coverage to the east and southeast of the center of storm. This is illustrated in Figure 6. In this part of the storm we knew for sure that low level clouds were being successfully targeted and tracked. The winds generated from these low level tracers looked quite good. We quickly discovered, however, that the winds were flagged by a quality control check that checks if the winds fall within the expected pressure range, which for visible winds is at or below 700hPa. Inspection of the retrieved pixel level cloud top pressures (not shown) over this area revealed cloud top pressures in the 200–400hPa range. Closer inspection of multi-spectral and IR



window imagery shown in Figure 7 clearly indicates the presence of thin cirrus overlapping the lower level cloud. The thin cirrus that overlapped the lower level clouds was clearly not identifiable by visible imagery alone. By using IR imagery, the presence of overlapping clouds (orange color) was correctly detected and flagged by the cloud type algorithm. As a means to retain the AMVs under this thin cirrus shield, we developed and tested an update to the AMV algorithm that takes advantage of the "OVERLAP" cloud type designation, estimated cloud emissivity, and opaque cloud height estimate provided by the cloud height algorithm. Thus, we use a simple IR window-based cloud height estimate for pixels flagged as having a "OVERLAP" cloud type designation and where the cloud emissivity is less than 0.20. Figure 8 shows the impact of this change. Note the increased coverage of low level winds east and southeast of the storm center.

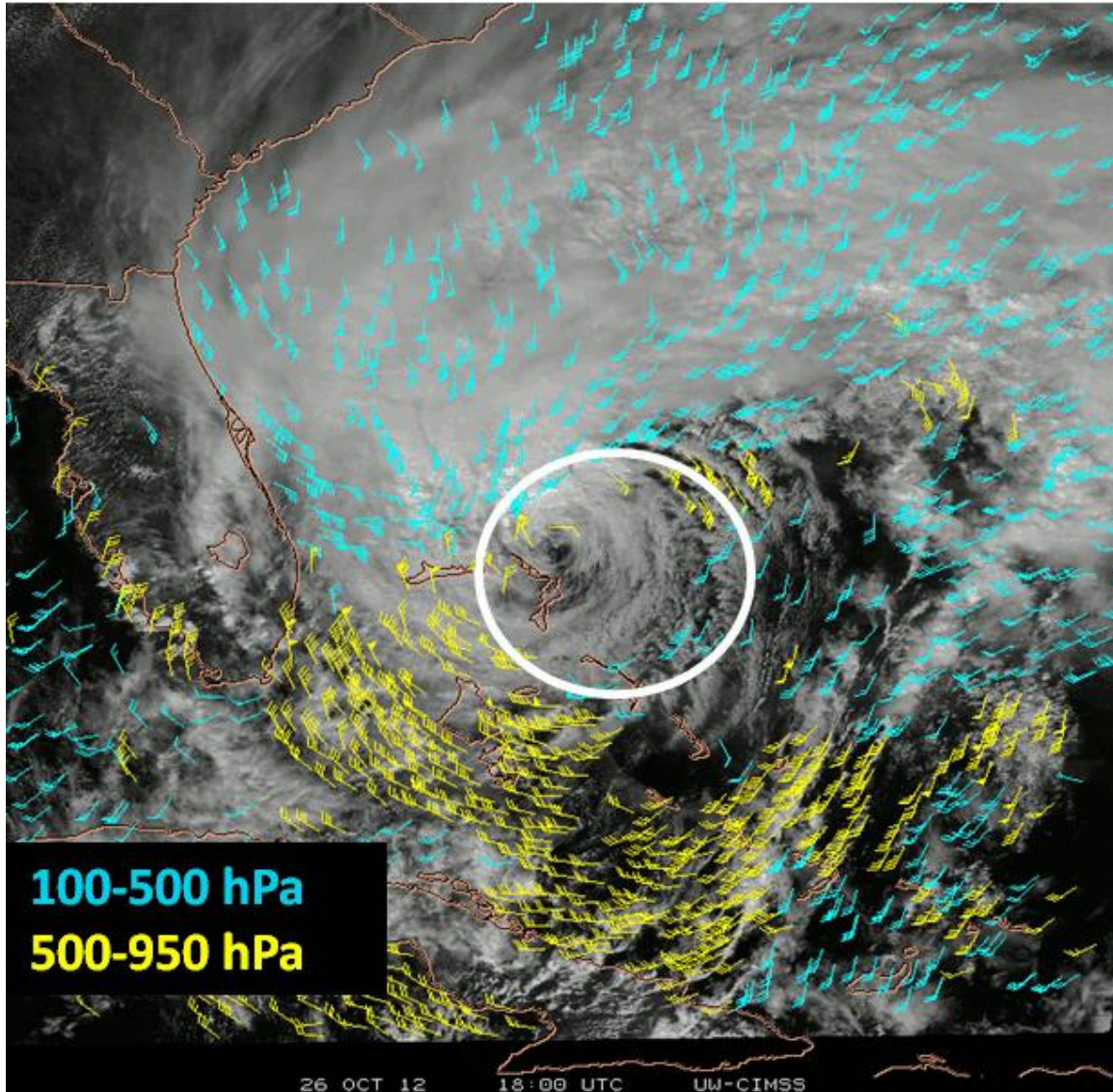


**Figure 6.** GOES-14 AMVs around Hurricane Sandy. Low level Visible AMVs (yellow) are at or below 700 hPa. Note the lack of low level visible AMVs just to the east and southeast of the center of Hurricane Sandy.

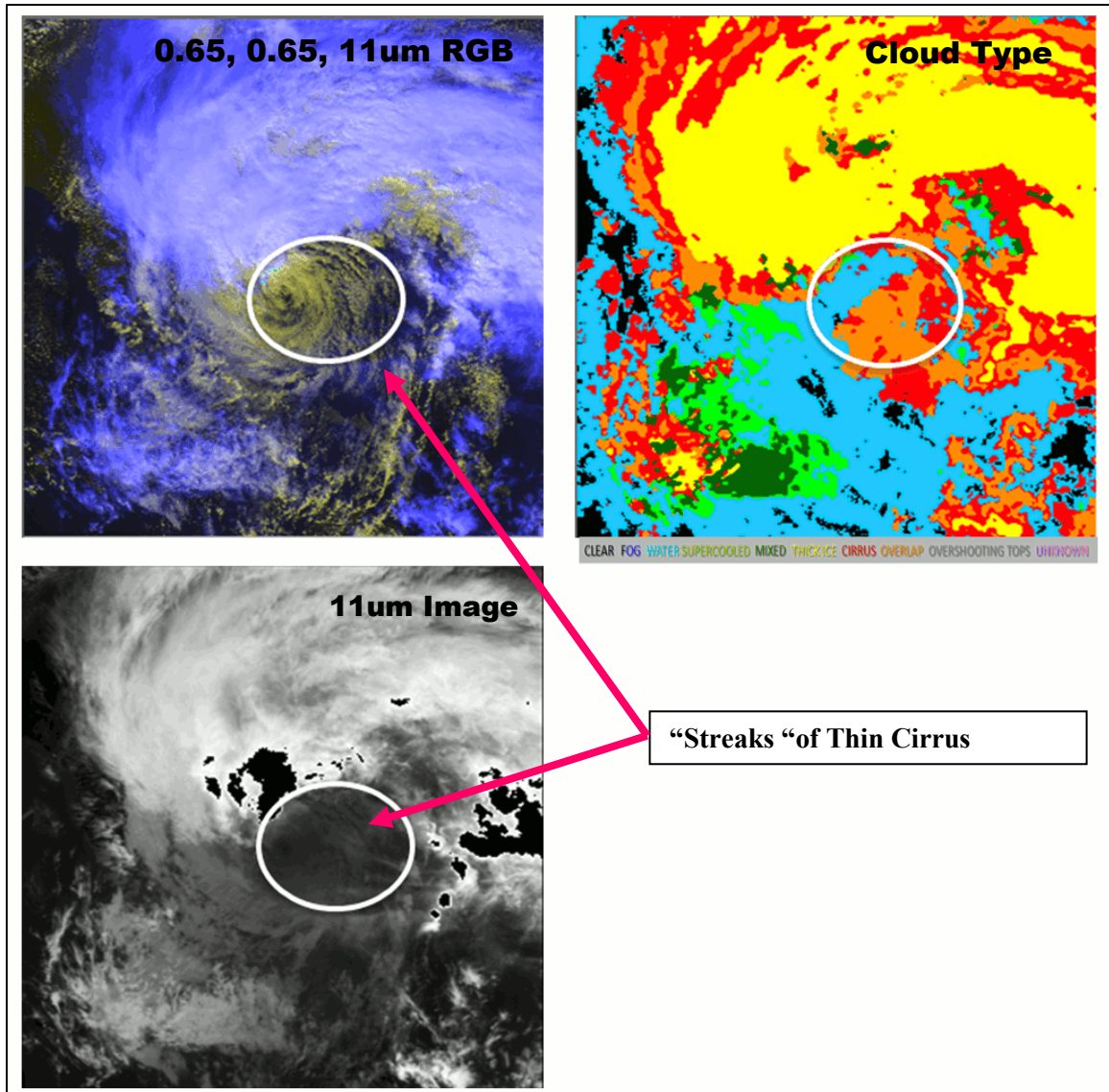


**Figure 7.** Assessment of GOES-14 imagery and cloud scene near the center of Hurricane Sandy. RGB fall color imagery (upper left), cloud type product (upper right), and 11um imagery (lower left). Figures courtesy of Mike Pavolonis (NESDIS).



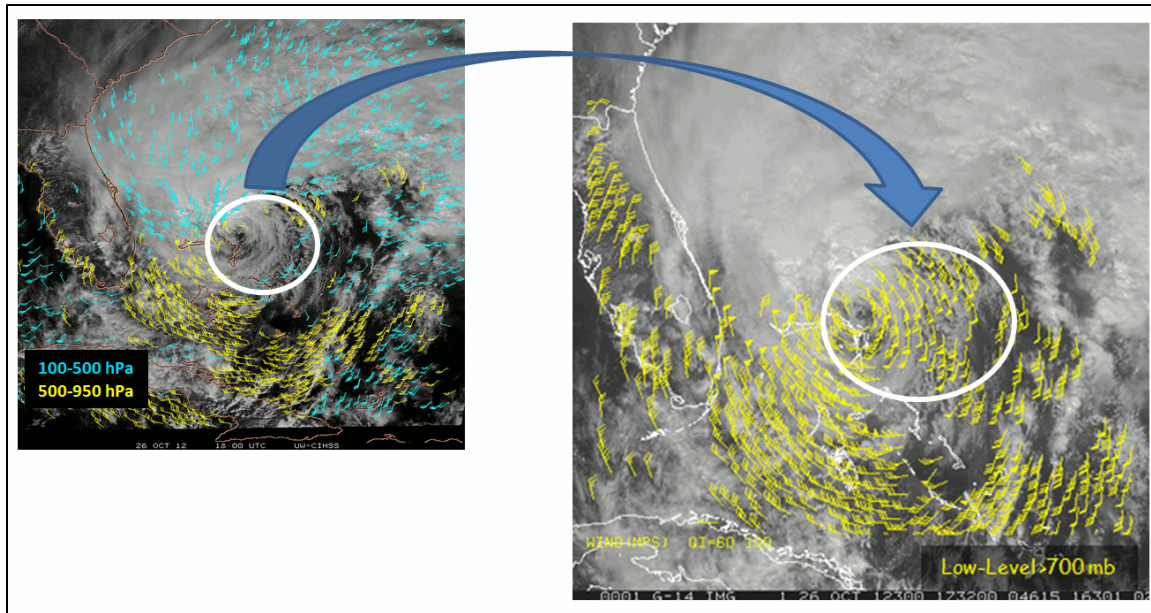


**Figure 8.** Increased coverage of low level visible AMVs (yellow) resulting from taking advantage of the “OVERLAP” cloud type designation, estimated cloud emissivity, and opaque cloud height estimate provided by the cloud height algorithm.

Additional testing was done with the full resolution test assess the impact of using more frequent imagery in the derivation of low level visible AMVs and the difference in AMV coverage when using conventional (e.g., non-nested) tracking versus nested tracking. Figure 9 illustrates some results of this testing. Note the large gains in AMV counts and geographic coverage as a result of using nested tracking versus conventional tracking. Not unexpectedly, the most significant gains in AMV counts and geographic coverage come with using higher temporal imagery in the AMV derivation process. In this case, images separated by 3 minutes were used to derive the visible AMVs. More testing is planned to derive VIS AMVs from imagery separated by 1-minute since we believe additional good AMVs can be retrieved. The increase in the AMV counts and geographic coverage achieved by leveraging the high temporal resolution imagery is important for furthering the utilization of these AMVs in Numerical Weather Prediction (NWP) and by NWS field forecasters.

Finally, the GOES-R AMV algorithm was tested with the 0.5 km resolution visible data from Himawari-8/AHI in the hopes of gaining valuable insight into the performance of the algorithm prior to the launch of GOES-R. Currently in NOAA Operations 1 km visible data from GOES is down-sampled to 2km before winds are generated. To better understand the impact of resolution on the new GOES-R algorithm, three tests were performed with the AHI 0.5 km visible data:

- The data was converted to 2km by sampling every fourth pixel of the full resolution image prior to generating winds.
- The data was converted to 2km by averaging (4x4 box) the full resolution image prior to generating winds
- The full resolution data was used without any downsampling of the data prior to generating the winds.

Results of testing (shown in Figure 10) suggest visible imagery should be processed at full resolution to capture the motion of the small scale cumulus clouds at low levels near the storm. If a reduction of the resolution is necessary it should be achieved through averaging and not through sampling.

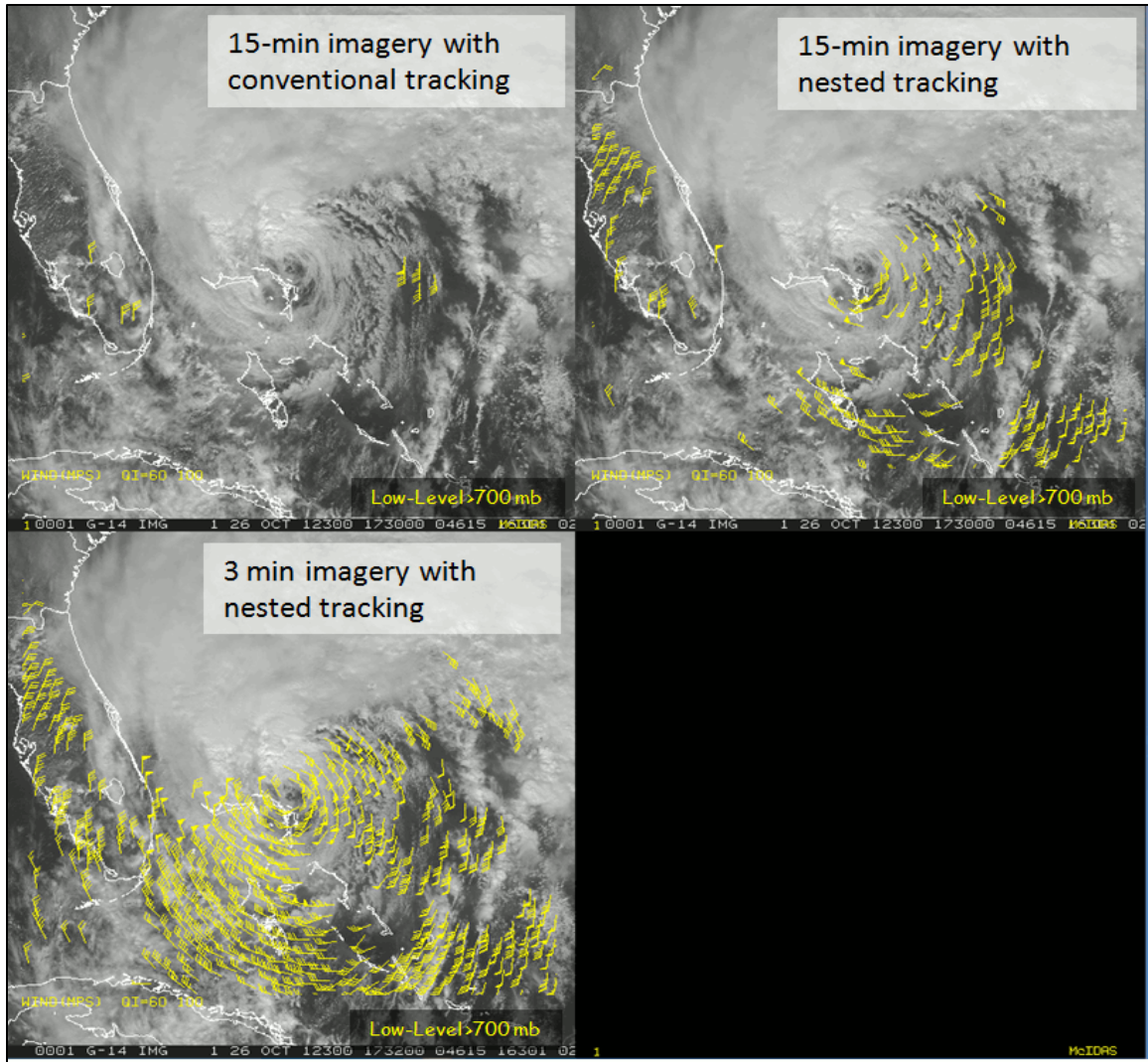


**Figure 9.** Coverage of low level visible AMVs over Hurricane Sandy resulting from using GOES-14 15-min imagery and conventional tracking (upper left), 15 –min imagery using nested tracking (upper right), and 3-minute imagery using nested tracking (lower left)

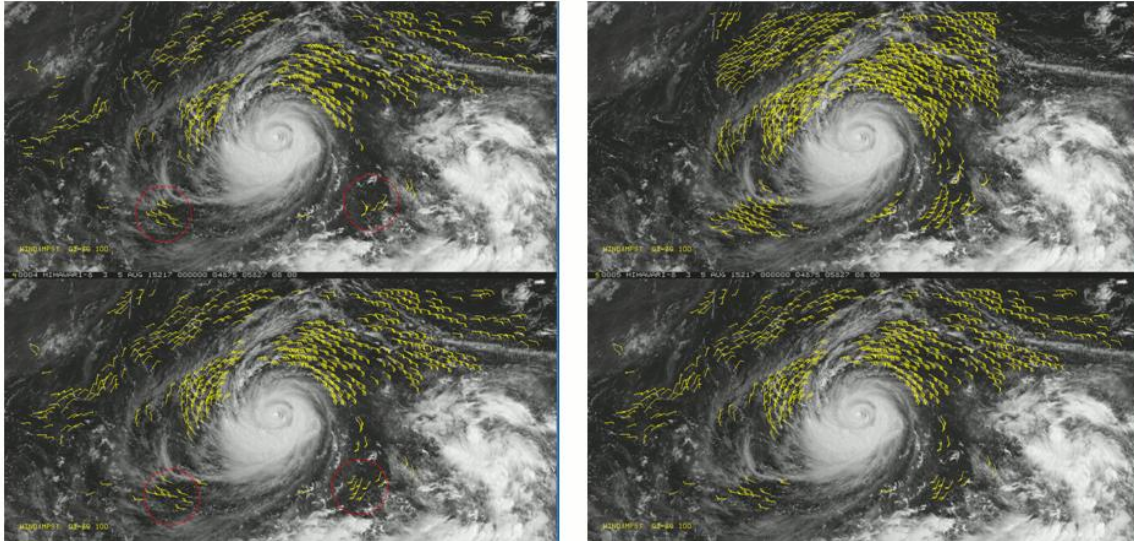


**Figure 10.** Winds generated using visible imagery reduced to 2km resolution by sampling (upper left) and 2km resolution by averaging (lower left). Note the improved coverage shown by red circles. Winds generated using full resolution (0.5km) imagery (upper right) and imagery reduced to 2km resolution by averaging (lower right).

## SUMMARY

The winds algorithm developed for GOES-R has undergone testing and validation using a number of different proxy data sources that include GOES-N/O/P, Meteosat/SEVIRI data, Terra/Aqua MODIS, NOAA/AVHRR, METOP/AVHRR, Soumi-NPP/VIIRS data, and more recently Himawari-8/AHI data. The GOES-14 super rapid scan (1-min) imagery and the Himawari-8/AHI imagery have been especially useful for testing and assessing the performance of the GOES-R winds algorithm. It's clear that utilization of the full resolution of the data (e.g. spatial, temporal, and spectral) will enable the generation of wind products with increased counts and significantly improved geographic coverage that should substantially increase the volume of information that will be available to the user community.

The availability of the Himawari-8/AHI imagery and its similarity to the GOES-R ABI have been of tremendous value for assessing the performance of the GOES-R winds algorithm prior to the launch of GOES-R. Comparisons of Himawari-8 AMVs generated via the GOES-R winds algorithm show very good agreement to radiosonde winds. This gives us very good confidence that the performance requirements levied on the GOES-R winds product will be met. More importantly, these results give us very good confidence that the GOES-R wind products will meet and exceed the needs of the user community.

## REFERENCES

Bessho, K., and Coauthors, 2016: An introduction to Himawari-8/9 - Japan's new-generation geostationary meteorological satellites. *J. Meteor. Soc. Japan.* , <http://doi.org/10.2151/jmsj.2016-009>.

Bresky, W., J. Daniels, A. Bailey, and S. Wanzong, 2012: New Methods Towards Minimizing the Slow Speed Bias Associated With Atmospheric Motion Vectors (AMVs). *J. Appl. Meteor. Climatol.*, 51, 2137-2151



Daniels, J., 2010: GOES-R Advanced Baseline Imager (ABI) Algorithm Theoretical Basis Document For Derived Motion Winds, GOES-R Program Office, 96 pp, [www.goes-r.gov](http://www.goes-r.gov).

Ester, M., H.-P. Kriegel, J. Sander and X. Xu, 1996: A Density-Based Algorithm for Discovering Clusters in Large Spatial Databases with Noise. *Proc. Second Intl. Conf. on Knowledge Discovery and Data Mining (KDD-96)*, Portland, OR, 226-231.

Heidinger, A. K., 2014: NOAA GOES-R AWG Cloud Height Algorithm (ACHA). *Proc. Twelfth Intl. Winds Workshop*, Copenhagen, Denmark, EUMETSAT.

Heidinger, A., 2010: GOES-R Advanced Baseline Imager (ABI) Algorithm Theoretical Basis Document For Cloud Height, GOES-R Program Office, 77 pp, [www.goes-r.gov](http://www.goes-r.gov).

Heidinger, A. K. and Pavolonis, M. J., 2009: Gazing at cirrus clouds for 25 years through a split window, Part 1: Methodology, *J. Appl. Meteorol. Clim.*, 48, 1100–1116, 2009.

Schmetz, J., P. Pili, S. Tjemkes, D. Just, J. Kerkmann, S. Rota, and A. Ratier, 2002: An Introduction to Meteosat Second Generation (MSG). *Bull. Amer. Meteor. Soc.*, 83, 977–992.

Schmit, T. J., P. Griffith, M. M. Gunshor, J. M. Daniels, S. J. Goodman and W. J. Lehair, 2016: A Closer Look at the ABI on GOES-R. *Bull. Amer. Meteor. Soc.* Accepted.

---

**Copyright ©EUMETSAT 2016**

This copyright notice applies only to the overall collection of papers: authors retain their individual rights and should be contacted directly for permission to use their material separately. Contact EUMETSAT for permission pertaining to the overall volume.

The papers collected in this volume comprise the proceedings of the conference mentioned above. They reflect the authors' opinions and are published as presented, without editing. Their inclusion in this publication does not necessarily constitute endorsement by EUMETSAT or the co-organisers

For more information, please visit [www.eumetsat.int](http://www.eumetsat.int)